Title: Exquisite specificity of Pks13 defines the essentiality of trehalose in mycobacteria

Authors: Yushu Chen[1], Justin Dao Tian Lim[1], Shu-Sin Chng[1,2]*

Affiliations:

[1] Department of Chemistry, National University of Singapore, Singapore 117543.

[2] Singapore Center for Environmental Life Sciences Engineering, National University of Singapore (SCELSE-NUS), Singapore 117456.

* To whom correspondence should be addressed. Email: chmchngs@nus.edu.sg

Classification: Biological Sciences (Biochemistry)

Keywords: outer membrane, polyketide synthase, mycolic acid, 6-azido-trehalose, trehalose dimycolate

Abstract

Mycolic acids (MAs) are the major component of the mycobacterial outer membrane, a key contributor to the intrinsic resistance of mycobacteria to external insults including multiple antibiotics. After being synthesized in the cytoplasm and before reaching the outer membrane, MAs are transported across the inner membrane in the form of an acylated sugar, generally believed to be trehalose monomycolates (TMMs). Whether trehalose is the only mycolate carrier during transport is under debate, and why this highly abundant disaccharide is essential for mycobacterial growth is unclear. To address these questions, we leveraged a trehalose auxotrophic *Mycobacterium smegmatis* strain to investigate the biosynthetic steps affording TMMs. We show that in addition to TMMs, MAs are also not produced in the absence of trehalose. This is likely due to a product inhibition mechanism where un-reduced MA precursors accumulate on Pks13, the protein catalyzing the ligation of mycolic acids and the sugar head group. We establish that the un-reduced mycolates could only be released by trehalose, revealing exquisite Pks13 specificity, and subsequently reduced by CmrA in vitro. Furthermore, only trehalose and its analogs can reactivate MA biosynthesis in cells. Finally, by replacing trehalose with a 6-deoxy analog in cells, we demonstrate that the cord factor trehalose dimycolate is dispensable for *M. smegmatis* growth in vitro. Our work gives a clear depiction of how TMMs are formed and provides a compelling reason for the essentiality of trehalose, shedding light on the development of future anti-mycobacterial strategies.

33 **Significance Statement**

34 Tuberculosis and other diseases caused by mycobacteria pose a persistent threat to human health and well-
35 being. The mycobacterial outer membrane is a highly impermeable barrier, conferring intrinsic resistance to
36 multiple antibiotics. How the biosynthesis of mycolic acids, the major component of the mycobacterial outer
37 membrane, is driven by trehalose is unknown. In this report, we study the molecular basis for the essentiality
38 of trehalose. We define the order of two critical steps in the mycolic acid biosynthetic pathway involving
39 trehalose and demonstrate the highly specific role that trehalose plays therein. This work answers key questions
40 in terms of outer membrane biogenesis in mycobacteria, providing a venue for the development of novel anti-
41 mycobacterial strategies.

42

43 **Introduction**

44 Mycobacteria are the cause of a number of severe human diseases, such as tuberculosis (TB) and leprosy.
45 There were more than 10 million new TB cases in a single year, and the disease alone claimed 1.1 million lives
46 in 2023 (1). This situation is compounded by the spread of multi-drug resistant (MDR) *Mycobacterium*
47 *tuberculosis* strains, and the higher risk of co-infection with TB in patients with human immunodeficiency
48 virus. Non-tuberculous mycobacterial infections, caused by *Mycobacterium abscessus* and related organisms,
49 have also been on the rise (2). The intrinsic resistance of mycobacteria to multiple antimicrobials and their
50 emerging resistance to current drugs mark an urgent need for the identification of new drug targets.

51 Mycobacteria possess a distinct cell envelope. Besides the cytoplasmic membrane (IM) and the
52 peptidoglycan (PG) cell wall, cells also contain an outer membrane (OM) bilayer, with the inner leaflet
53 covalently linked to arabinogalactan (AG) polysaccharides extending outward from PGs (3, 4). The essential
54 mycobacterial OM serves as an effective permeability barrier (5), which is largely contributed by the abundance
55 of tightly packed mycolic acids (MAs) in the bilayer. These MAs are either linked to AG-PG as the entire inner
56 leaflet (termed mycolyl-AGP or mAGP), or found as free lipids at the outer leaflet in the forms of trehalose
57 monomycolates (TMMs) and trehalose dimycolates (TDMs). MAs are 2-alkyl, 3-hydroxyl, very long chain,
58 branched fatty acids (C_{58}-C_{86}) present in mycobacteria, as well as phylogenetically related genera (6, 7). They
59 comprise the shorter α branch (C_{22}-C_{24}) and the longer meromycolate chain (C_{36}-C_{60}), which are synthesized
60 by a single FAS-I protein and a multi-protein FAS-II system, respectively (Fig. 1) (8). Different functional
61 groups are introduced onto the meromycolate chain, giving rise to different MA classes - *M. tuberculosis*
62 produces α-, methoxy-, and keto-MAs while *Mycobacterium smegmatis* contains α- (C_{72}-C_{84}) and epoxy-MAs,
63 in addition to α'-MAs with a much shorter overall chain length (C_{58}-C_{66}) (8). Fully extended α-alkyl chains are
64 carboxylated, and then condensed with meromycolate chains by polyketide synthase 13 (Pks13) (9), affording
65 the MA precursors α-alkyl-β-ketoacids that are reduced by CmrA, (10) and esterified by trehalose to form

66 TMMs (11); the order of these final two reactions in cells remain to be clarified (Fig. 1). TMMs are generally
67 believed to be the final MA product in the IM and are continuously transported across the cell envelope to build
68 the OM. The transport process is largely elusive, however, except for the identification of MmpL3 as the TMM
69 flippase at the IM (12), and Ag85 enzymes as the mycolyltransferases for mAGP and TDM formation at the
70 OM (13). Targeting the MA biosynthetic and transport pathways has proven to be an important anti-
71 mycobacterial strategy, exemplified by the prevailing application of isoniazid, a first-line anti-TB drug
72 targeting FAS-II (14).

73 There are knowledge gaps in mycolate biosynthesis that would be important for our understanding of
74 mycobacterial physiology. One intriguing question is why trehalose is an essential metabolite for growth (15).
75 It has been proposed that the role of trehalose as the final acceptor for MAs accounts for its essentiality.
76 However, in vitro evidence suggested that Pks13 is not strictly specific for trehalose; several other mono- and
77 disaccharides can release α-alkyl-β-ketoacids, albeit non-native short chain versions, from the enzyme to form
78 the corresponding ester (11). Glycerol and glucose monomycolates have also previously been detected in
79 lipidomic analyses (16, 17), although it is unclear whether they are derived directly from Pks13 or via mycolyl
80 transfer reactions catalyzed by Ag85s, leading to sugar headgroup exchange (18). Therefore, is the
81 predominance of TMM as the mycolate carrier in cells due to the high abundance of trehalose, or the hitherto
82 unknown in vivo specificity of Pks13, which may then explain trehalose essentiality?

83 To elucidate acceptor specificity in cells, we need to devise a way to study the release of native mycolates
84 from Pks13 by trehalose (or other sugars). We reasoned that we might be able to accumulate mycolates or its
85 precursors on Pks13 by depleting the acceptor and stalling release. In this study, we exploited a trehalose
86 auxotrophic *M. smegmatis* strain (TKO) lacking all three trehalose biosynthetic pathways (19), namely the
87 OtsAB, TreYZ, and TreS pathways (20) (Fig. 1). This strain can only grow in the presence of exogenous
88 trehalose actively taken up via the LpqY-SugABC ATP-binding-cassette (ABC) transporter (21). We conducted

89 extensive lipid profiling of TKO cells depleted of trehalose, and reconstituted the final steps leading to TMM
90 formation using native substrates from endogenously purified Pks13. We show that upon trehalose depletion,
91 cells stop synthesizing mature MAs and TMMs, likely due to product accumulation on Pks13 that prevents
92 further substrate turnover. Interestingly, only adding back trehalose, but not other sugars, can reactivate MA
93 biosynthesis. Furthermore, we demonstrate that only trehalose can be used by purified Pks13 to release
94 unreduced mycolates, for subsequent reduction by CmrA. Our work highlights the exquisite specificity of
95 trehalose as the mycolate acceptor in cells, providing a molecular basis for its essentiality in mycobacteria.
96

97 **Results**

98 **Trehalose depletion causes cessation of de novo MA biosynthesis**

99 To study MA biosynthetic steps involving Pks13 and trehalose in mycobacteria, we first profiled newly
100 synthesized lipids upon trehalose depletion in the *M. smegmatis* Δ*otsA*Δ*treYZ*Δ*treS* (TKO) trehalose auxotroph.
101 TKO cells stopped growing after 48 h (*SI Appendix*, Fig. S1*A*), when we showed that intracellular trehalose
102 was fully depleted (*SI Appendix*, Fig. S1*B*). At that point, cells were labeled with [^{14}C]-acetate, and newly
103 synthesized lipids in the forms of total extractable lipids (containing TMMs) or total mycolates (esterified as
104 MA methyl esters, MAMEs) were isolated and analyzed by thin layered chromatography (TLC). As expected,
105 mutant cells depleted of trehalose (dTKO cells) were deficient in TMM formation (Fig. 2*A*). Surprisingly,
106 trehalose depletion also resulted in essentially no newly-synthesized mycolates (Fig. 2*B*), indicating that MA
107 biosynthesis was possibly disrupted at steps before TMM formation. When the same cells were exogenously
108 re-supplemented with trehalose during [^{14}C]-labeling, both MA biosynthesis and TMM formation were
109 restored (Fig. 2). Importantly, restoration of MA biosynthesis was not inhibited by several antibiotics that
110 stopped cellular growth (*SI Appendix*, Fig. S2), suggesting that the cessation of MA synthesis was not due to
111 growth arrest caused by lack of trehalose. The newly-synthesized MAs and TMMs, immediately upon trehalose

112 re-supplementation, exhibited a higher α' (C_{58-66}) to α (C_{72-84}) ratio than those in wild-type cells (Fig. 2*A* and
113 *B*), a phenomenon also observed in cells when FAS-II was perturbed (*SI Appendix*, Fig. S3) (22-24).
114 Transcriptomic analyses revealed that genes in the *fabD-acpM-kasA-kasB-accD6* operon, but not those
115 encoding other FAS-II components, were up-regulated in trehalose-depleted cells (Fig. 3*A*), consistent with
116 FAS-II perturbation. Furthermore, we observed up-regulation of the *acpS-fas*, *accD4-pks13-fadD32*, and
117 *iniBAC* operons (Fig. 3*A* and *SI Appendix*, Fig. S4), perhaps a result of stalled MA biosynthesis, reminiscent
118 of cellular responses of *M. tuberculosis* to FAS-I/II inhibitors (cerulenin, thiolactomycin and isoniazid) (25,
119 26). It is likely that TKO cells exhibit different metabolic states with or without trehalose. Following prolonged
120 trehalose re-supplementation, the cellular transcriptomic profile of TKO cells became more similar to wild type
121 cells (Fig. 3*A*). In addition, the ratio of α'- to α-mycolates was fully restored in a manner dependent on active
122 transcription and translation (Fig. 3*B–D*). Taken together, our results establish that trehalose is required for de
123 novo MA biosynthesis.
124

125 **Trehalose depletion causes accumulation of keto-mycolates on Pks13 that must be released and reduced**
126 **sequentially to form TMMs**

127 Both mycolate biosynthesis and TMM formation were abolished in trehalose-depleted cells. We reasoned
128 that these observations may indicate accumulation of lipids on Pks13, which prevents further turnover of
129 mycolate substrates. To test this idea, we labeled *M. smegmatis* dTKO cells with [^{14}C]-acetate and analyzed
130 the whole cell protein profile via SDS-PAGE. Notably, a radioactive band showed up at ~200 kDa (*SI Appendix*,
131 Fig. S5), which is consistent with the size of Pks13 (197.1 kDa). The radioactivity on the band could be reduced
132 by treatment with either trehalose or the mycolate biosynthesis inhibitor isoniazid (*SI Appendix*, Fig. S5),
133 suggesting that the labeled band contains mycolate-related lipids. We next expressed C-terminally His-tagged
134 Pks13 from an integrative plasmid, and isolated it from [^{14}C]-acetate-labeled dTKO cells via affinity

135 purification. Remarkably, we detected significant radioactivity on Pks13-His from these cells (Fig. 4*A*); the
136 signal was much weaker when the same cells had been treated with trehalose or isoniazid (Fig. 4*B* and *C*).
137 These results indicate that mycolate precursors accumulate on Pks13 upon trehalose depletion, likely
138 accounting for why de novo biosynthesis of mycolates is abolished in the absence of trehalose.

139 To elucidate what lipid species may have accumulated on Pks13, we attempted to use trehalose to release
140 lipids from affinity-purified Pks13-His in vitro. Interestingly, trehalose indeed facilitated the formation of a
141 new extractable lipid species in the reaction mixture. The lipid migrated slightly faster than TMM on normal-
142 phase TLC, suggesting that it is a less polar derivative of the latter (Fig. 4*D*). By comparing the mobility of
143 this lipid to TMM species synthesized in a strain lacking the reductase CmrA (10), we assigned it to be trehalose
144 α-alkyl-β-ketomeromycolate, the unreduced keto form of TMM (TMM*k*). The release of the α-alkyl-β-
145 ketomeromycolate precursor to form TMM*k* is believed to be catalyzed by the thioesterase domain of Pks13.
146 While this reaction can happen in the absence of the ketoreductase CmrA both in vitro (11) and in cells (27), it
147 is not clear whether the reduction step actually takes place before or after the release. Notably, the observed
148 accumulation of α-alkyl-β-ketomeromycolates in the absence of trehalose demonstrates the inability of
149 endogenous CmrA to reduce this precursor directly on Pks13. Consistent with this idea, only when we also
150 added purified CmrA and NADPH during the reaction, we observed the conversion of TMM*k* to mature TMM
151 (Fig. 4*E–G* and *SI Appendix*, Fig. S6). A mutation at the putative CmrA active site ($CmrA^{Y157F}$) reduced the
152 conversion significantly. Therefore, we have effectively recapitulated in vitro the final release and reduction
153 steps in the formation of TMM. We conclude that trehalose release of mycolates from Pks13 allows subsequent
154 CmrA reduction to form TMMs.

155

156 **Release of native ketomycolates from Pks13 is highly specific to trehalose**

157 Having established that unreduced MA precursors can be released from Pks13 and esterified by trehalose

158 in vitro, we further explored if other sugars could act as MA acceptors. In an earlier study, unreduced MA
159 analogs (C_{30}) could be synthesized in vitro and released from recombinant Pks13 by a few mono- and
160 disaccharides other than trehalose, including mannose, allose, maltose, and most prominently glucose (11) (Fig.
161 5*A*). Surprisingly, none of these sugars facilitated formation of ketomycolate sugar esters when added to Pks13
162 endogenously purified from dTKO cells (Fig. 5*B*); we reasoned that the longer chain length of native
163 ketomycolates can in fact contribute to the sugar specificity of the MA acceptor. We also tested other trehalose
164 analogs in the release assay. Notably, 6-azido-trehalose, but not 6,6'-diazido-trehalose, could drive the
165 formation of 6-azido-TMM*k* in the reaction mixture, consistent with the requirement of a free 6'-OH group;
166 this observation also corroborates that α-alkyl-β-ketomeromycolates accumulated on Pks13 in the absence of
167 trehalose. The identity of the 6-azido-trehalose-released product was assigned based on its similar migration
168 on TLC when compared to 6-azido-TMM*k* produced in Δ*cmrA* cells fed with 6-azido-trehalose (*SI Appendix*,
169 Fig. S7). To extend the finding on acceptor specificity, we next examined the ability of the various sugars in
170 activating de novo mycolate biosynthesis when re-supplemented to dTKO cells. Remarkably, only 6-azido-
171 trehalose (in addition to trehalose) enabled the formation of newly-synthesized MAs (Fig. 5*C*), and thus TMMs
172 (*SI Appendix*, Fig. S8*A*), consistent with its ability to release accumulated precursors from Pks13. We confirmed
173 the assignment of 6-azido-TMMs hence formed by demonstrating its reactivity with an alkyne-containing
174 probe via click chemistry (*SI Appendix*, Fig. S8*B*) (28). We conclude that Pks13 exclusively uses trehalose as
175 the MA acceptor in cells, which can explain the essentiality of trehalose in mycobacteria.
176

177 **TDM is dispensable for *M. smegmatis* growth in vitro**

178 It is intriguing that 6-azido-trehalose is able to release mycolate precursors from Pks13 (Fig. 5*B*) and
179 facilitate continuous MA biosynthesis (Fig. 5*C*). In fact, we found 6-azido-trehalose alone could support the
180 growth of TKO cells, albeit at a slower rate than that supported by the same amount of trehalose (Fig. 6*A*). This

181 observation implies that *M. smegmatis* cells can survive without TDM; in the trehalose auxotrophic strain
182 grown in 6-azido-trehalose, mAGP but not TDM could be formed, since the mycolyl chain from 6-azido-TMM
183 can still be transferred to AGs but not another 6-azido-TMM molecule lacking the 6-OH group (Fig. 1). Using
184 [^{14}C]-acetate lipid profiling, we confirmed that 6-azido-trehalose-fed TKO cells made mAGP but not TDM
185 (Fig. 6*B*). Notably, we did not detect any major difference in drug sensitivity between TKO cells with and
186 without TDM (*SI Appendix*, Table S1). Therefore, we assert that the TDM, despite its key role in pathogenicity
187 as the cording factor (29), is not essential for growth and OM permeability function of *M. smegmatis* in vitro,
188 and possibly other mycobacteria.
189

190 **Discussion**

191 By using a trehalose auxotrophic strain, we have demonstrated that trehalose depletion abolishes de novo
192 MA biosynthesis, likely due to intermediates accumulating on Pks13. In addition, we have established that
193 Pks13 is highly specific, and only uses trehalose to release β-keto-mycolates from its thioesterase domain.
194 Furthermore, we have found that CmrA is unable to reduce β-keto-mycolates on Pks13 itself in cells, a process
195 that occurs only after the formation of TMM*k*. Our study has recapitulated the final steps in the MA biosynthetic
196 pathway with native substrates, and the details therein, revealing why the specific disaccharide trehalose is
197 essential in mycobacteria.

198 Our findings that trehalose is a highly specific acceptor for mycolates on Pks13 differ from an earlier study
199 in vitro (11). One key factor that may account for this difference is the use of short mycolate analogs in that
200 study, compared to the tracking of native substrates accumulating on Pks13 here, both in cells and in vitro. The
201 thioesterase domain in polyketide synthases (PKSs) often serves as a chain length regulator or a proof-reading
202 enzyme: in the case of shorter products formed on the acyl carrier protein domain, the thioesterase domain may
203 remove the acyl chain to prevent blockage of the synthetic cascade (30). We therefore reason that the use of

204 shorter mycolate analogs may have rendered Pks13 more promiscuous in the choice of the sugar acceptor.
205 Furthermore, it is conceivable that high specificity for trehalose as the acceptor for mycolates is important for
206 streamlining downstream processes, at least for transport. Specifically, the exquisite synthesis of TMM
207 circumvents the need for multiple redundant transporters to accommodate different hydrophilic sugar
208 headgroups during flipping across the IM, and/or transport to the OM (31).

209 Mycobacteria leverage multiple PKSs for the biosynthesis of complex lipids to build their unique OM (32).
210 Among them, Pks13 is essential for mycobacterial growth (9) and has been revealed as the target of a few hit
211 and lead compounds (33-35). It had not been established whether the reduction of ketomycolates by CmrA
212 happens before or after the release and esterification by trehalose in the TMM biosynthesis pathway. Cells
213 lacking CmrA still produce TMM*k* (10), indicating that ketomycolates can be released from Pks13 by
214 endogenous trehalose. Notably, we have now demonstrated that cells depleted of trehalose accumulate
215 ketomycolates on Pks13, revealing that endogenous CmrA cannot reduce this precursor. We have further shown
216 that CmrA-mediated reduction would proceed after the formation of TMM*k* in vitro, establishing that reduction
217 of ketomycolates only takes place after release from Pks13 by trehalose. Such post-release reduction contrasts
218 from most other PKSs where keto-reduction steps occur before final release (36). Given that β-keto-acids can
219 undergo spontaneous decarboxylation reactions, we speculate that preventing reduction of ketomycolates in
220 the absence of trehalose may provide an avenue for degradation and re-assimilation, especially in the context
221 of corynebacteria where MAs are non-essential (37).

222 We have shown that trehalose is required for de novo MA biosynthesis. A simple explanation is that the
223 accumulation of intermediates on Pks13 without trehalose prevents reduction by CmrA, and thus formation of
224 mature mycolates. However, the impact of such accumulation on substrate loading and condensation on Pks13,
225 or on upstream MA biosynthetic steps, cannot be ruled out. It is also not clear how inhibition of MA
226 biosynthesis upon trehalose depletion results in a transcriptional response that up-regulates *acpS-fas*, *fabD*-

227 *acpM-kasA-kasB-accD6* and *accD4-pks13-fadD32* operons, which likely accounts for the high α'- to α-MA
228 ratio when trehalose was re-supplemented. Interestingly, these transcriptomic changes are highly similar to
229 those reported for drugs inhibiting FAS-I or II enzymes that are responsible for mycolic acid biosynthesis, but
230 not other envelope pathways (25), suggesting that the changes were elicited specifically by lack of mature
231 mycolates. While it is clear that cells depleted of trehalose exhibit general envelope stress, evidenced by up-
232 regulation of the *iniBAC* operon (26), we postulate that mycobacteria may have yet-to-be-identified
233 mechanisms to sense mycolates in the cell, so as to counteract defects in overall envelope assembly. This would
234 be analogous to how Gram-negative bacteria deploy various LPS sensing mechanisms to ensure proper OM
235 assembly (38).

236 Finally, we have also been able to show that TDM is not essential for in vitro mycobacterial growth. While
237 other studies have alluded to this idea, it was never before possible to remove TDM completely (39, 40); this
238 limitation may also impact the interpretation of in vivo studies that ascribed TDM as a key virulence factor and
239 immune response modulator (41, 42). A trehalose auxotrophic strain supplemented with 6-deoxy-trehalose
240 analogs may thus be useful for future studies on TDM in vivo. Our study provides valuable insights into the
241 formation of MA, TMM and TDM, and serves as a foundation for the development of new anti-mycobacterial
242 drugs, especially against Pks13.

243

244 **Supporting Information**

245 - Detailed materials and methods.
246 - Figures S1-S8 and Table S1

247

248 **Acknowledgments**

249 We thank Prof. Carolyn Bertozzi (Stanford University) and Prof. Rainer Kalscheuer (Heinrich-Heine-

Universität Düsseldorf) for providing the TKO strain, as well as various single and double mutants in trehalose biosynthesis. 6-azido-trehalose is a kind gift from Prof. Benjamin Swarts (Central Michigan University). We thank Dr. Qiping Liu (Chemical, Molecular and Materials Analysis Centre, National University of Singapore) for the guidance and help with GC-MS. Library preparation and RNA sequencing was done by the integrated Genome Analytics Platform at the Genome Institute Singapore. This project was funded by Singapore Ministry of Education Academic Research Fund Tier 2 grant MOE-000116 (S.-S.C.).

Author Information

Corresponding author: Shu-Sin Chng. Email: chmchngs@nus.edu.sg

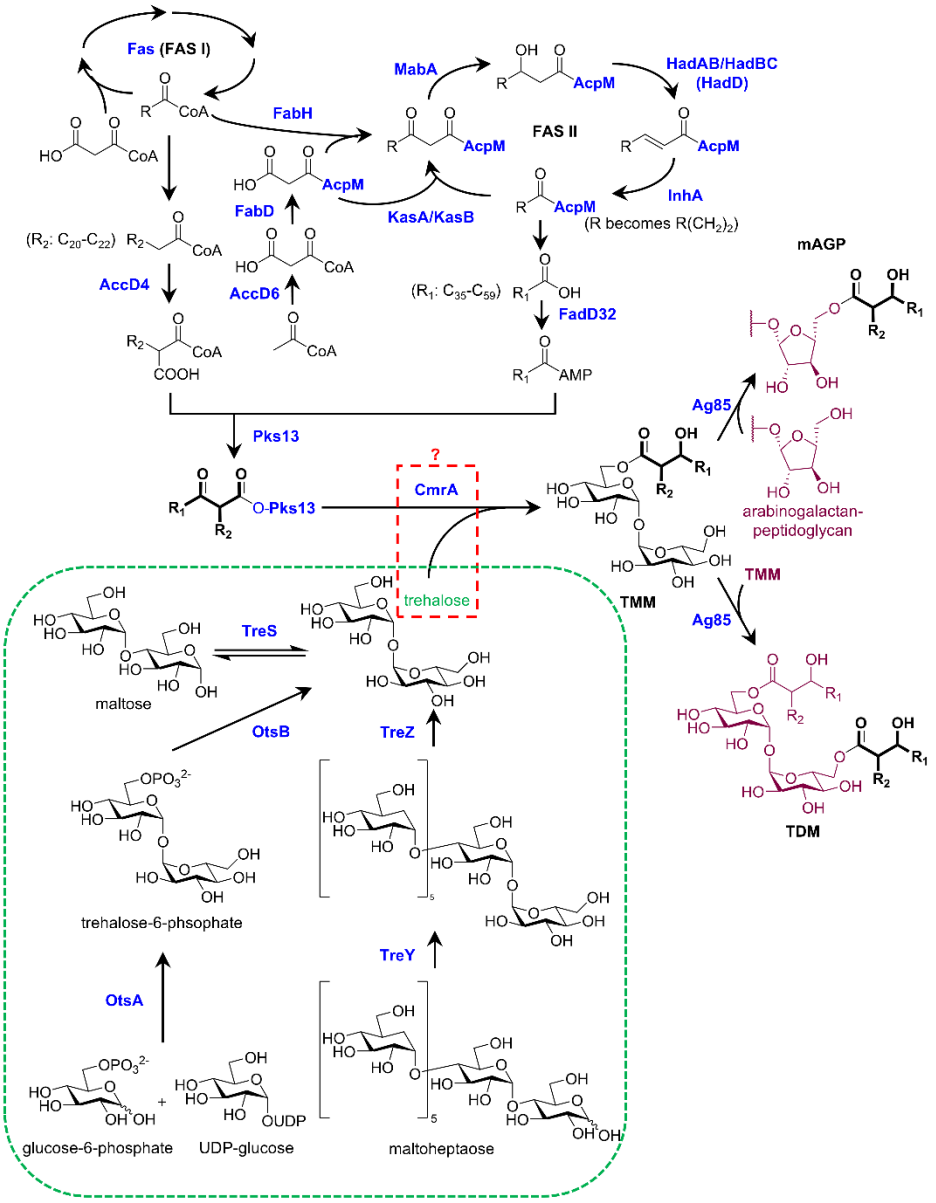

Figure 1. Biosynthetic pathways for trehalose, MAs, TMMs, TDMs and mAGP. Short chain α-branch fatty acids and long chain meromycolates are synthesized by FAS-I and FAS-II, respectively, and then condensed to give α-alkyl-β-ketomeromycolates on Pks 13. Subsequent trehalose-mediated release and CmrA-dependent reduction (in unknown order) of Pks13-linked α-alkyl-β-ketomeromycolates yields TMMs, which are transported to the OM and converted into TDMs and mAGP by Ag85 enzymes. FAS, fatty acid synthase.

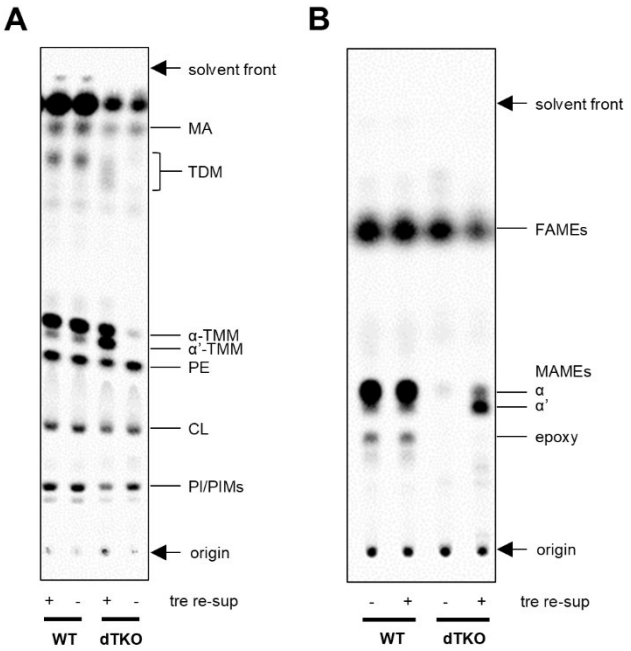

Figure 2. Trehalose is required for TMM formation and de novo MA biosynthesis. (*A*) TLC analysis of [^{14}C]-labeled lipids extracted from *M. smegmatis* WT or dTKO (TKO depleted of trehalose) cells, with (+) or without (-) trehalose re-supplementation (tre re-sup). Developing solvent: chloroform:methanol:water 30:8:1. CL, cardiolipin; PE, phosphatidylethanolamine; PI, phosphatidylinositol; PIMs, phosphatidylinositol mannosides. (*B*) TLC analysis of [^{14}C]-labeled fatty acids liberated from indicated strains, esterified as methyl esters. Three MAME species, α-, α'-, and epoxy-, were observed. Developing solvent: three times in hexane:ethyl acetate 95:5. TKO cells were depleted of trehalose (dTKO) prior to labelling and lipid extraction. FAME, fatty acid methyl ester; MAME, mycolic acid methyl ester. For samples on the same TLC plate, the same amount of radioactivity was loaded. The TLC plates were visualized by phosphor imaging.

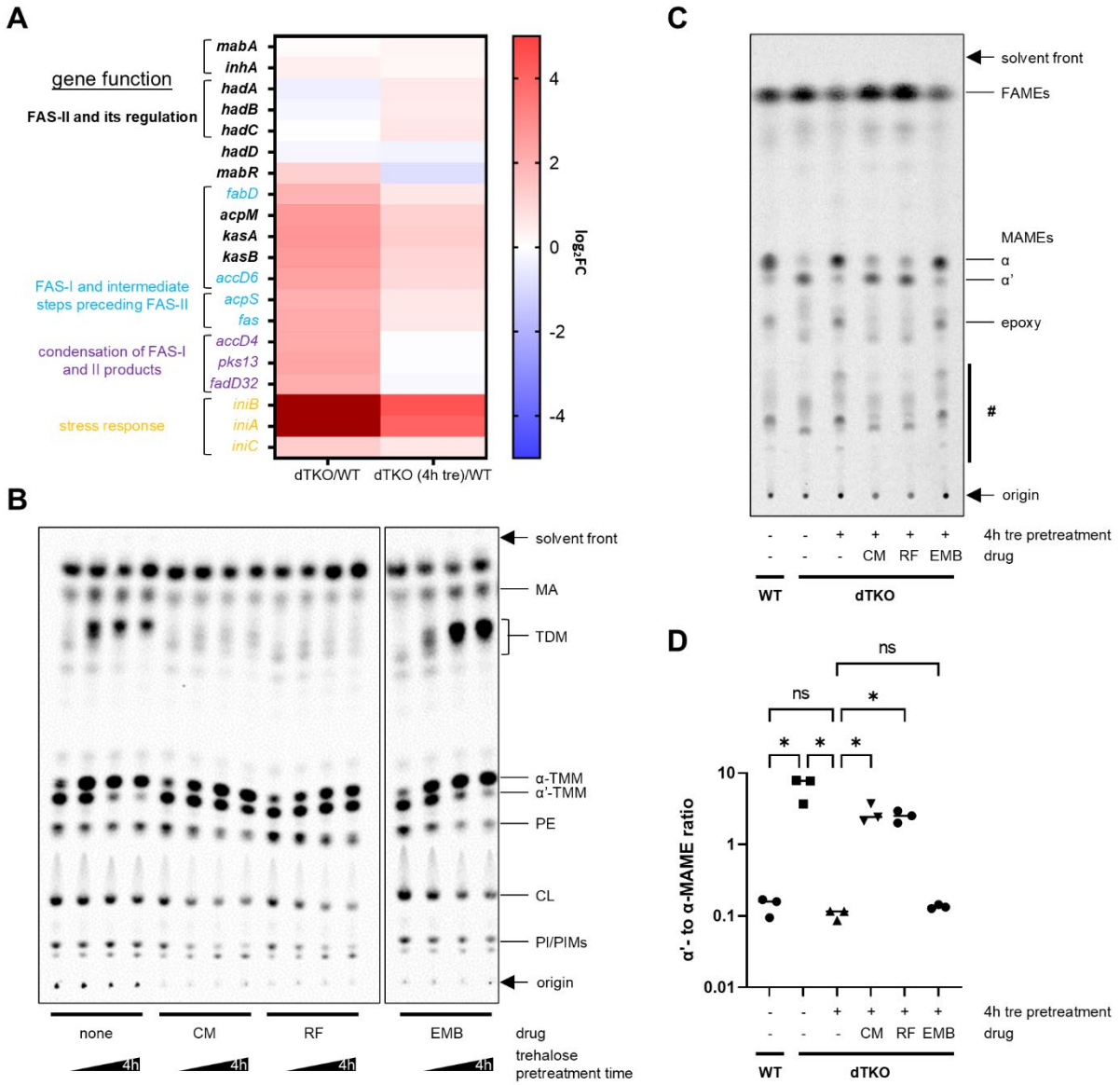

Figure 3. Trehalose-depleted TKO cells are in a distinct metabolic state. (*A*) Heat maps representing changes in transcript levels of indicated genes, either involved in MA metabolism or reportedly induced by FAS inhibitors, when comparing dTKO cells (trehalose-depleted TKO), or dTKO cells with trehalose re-supplementation (4h tre), to WT cells. Three biological replicates were used for each condition. FC, fold change. Maroon color on the heat map (*iniA* and *iniB* in the dTKO/WT column) indicates $\log_2 FC > 4$. Genes in the same bracket are in the same operon. (*B*) TLC analysis of [^{14}C]-labeled lipids extracted from dTKO cells pretreated with 20 μM trehalose in the presence of different drugs for extended periods of time (0, 1, 2.5 or 4

283 h) before radiolabeling with [^{14}C]-acetate. Developing solvent: chloroform:methanol:water 30:8:1.
284 Chloramphenicol (CM), rifampicin (RF) and ethambutol (EMB) inhibit translation, transcription and AG
285 biosynthesis, respectively. CL, cardiolipin; PE, phosphatidylethanolamine; PI, phosphatidylinositol; PIMs,
286 phosphatidylinositol mannosides. (*C*) TLC analysis of [^{14}C]-labeled total acyl methyl esters derived from
287 dTKO cells pretreated with 20 μM trehalose in the presence of different drugs for 4 h before radiolabeling with
288 [^{14}C]-acetate. "#" denotes lipids with unknown identities. Developing solvent: three times in hexane:ethyl
289 acetate 95:5. For samples on the same TLC plate, the same amount of radioactivity was loaded. The TLC plates
290 were visualized by phosphor imaging. (*D*) Quantification of α'- and α-MAME in (*C*). Each data point (mean
291 ± SD) represents the results from three biological replicates. ns, not significant; *, $p < 0.05$. FAME, fatty acid
292 methyl ester; MAME, mycolic acid methyl ester.

293

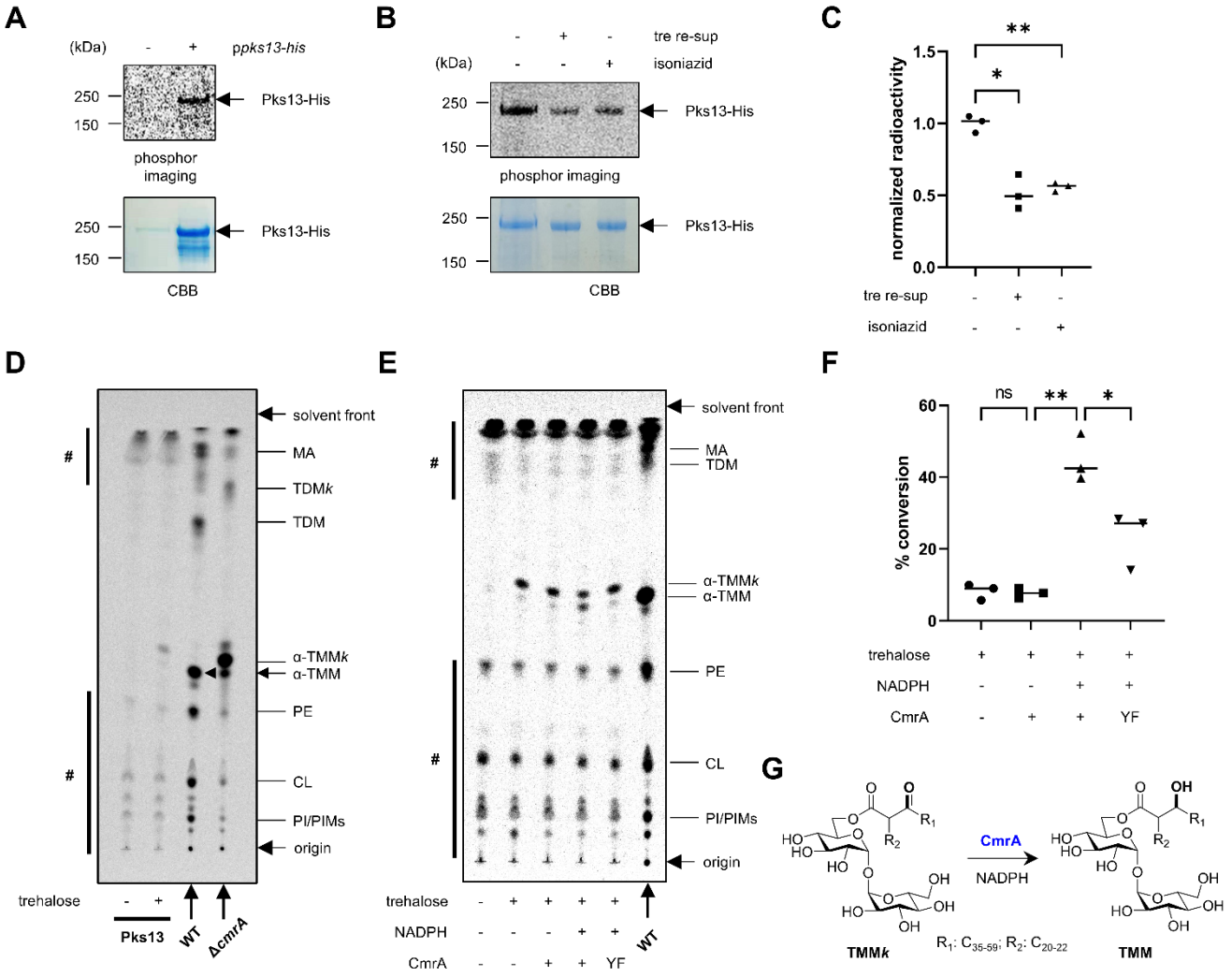

Figure 4. Unreduced mycolates accumulate on Pks13 upon trehalose depletion. *(A)* and *(B)* SDS-PAGE analyses of Pks13-His affinity purified from dTKO cells harboring empty vector or pJEB402-*pks13-his*$_8$ grown in the presence of [^{14}C]-acetate. The gel was visualized by phosphor imaging (top) and Coomassie brilliant blue staining (CBB; bottom). tre re-sup, trehalose re-supplementation. In *(B)*, trehalose (tre re-sup) or isoniazid was added together with [^{14}C]-acetate. (*C*) Quantification of the Pks13-associated lipids in different conditions in (*B*). Each data point (mean ± SD) represents the results from three biological replicates. *, $p < 0.05$; **, $p < 0.01$. (*D*) and (*E*) TLC analyses of [^{14}C]-labeled lipids extracted from affinity-purified Pks13-His subjected to (*D*) in vitro mycolate release by trehalose, and (*E*) reduction by CmrA. Lipids extracted from WT and Δ*cmrA*

303 cells were used as references for migration positions of α-TMM and α-TMM*k*, respectively. For clarity, α'-
304 TMM and α'-TMM*k* (spots immediately below corresponding α-TMM and α-TMM*k*) are not labelled for these
305 samples. CL, cardiolipin; PE, phosphatidylethanolamine; PI, phosphatidylinositol; PIMs, phosphatidylinositol
306 mannosides. For in vitro samples, the top and bottom spots (#) on the TLC other than TMM*k* and TMM are
307 present even in the absence of trehalose and are likely non-specific lipids bound to TALON resin used for
308 affinity purification of the protein. Developing solvent: chloroform:methanol:water 30:8:1. The TLC plates
309 were visualized by phosphor imaging. (*F*) Quantification of the conversion of trehalose mono-β-ketomycolate
310 (TMM*k*) to TMM in different conditions in (*E*). Each data point (mean ± SD) represents the results from three
311 biological replicates (see *SI Appendix*, Fig. S6 for other replicates). YF, CmrA containing a Y157F mutation.
312 ns, not significant; *, $p < 0.05$; **, $p < 0.01$. (*G*) Reaction scheme illustrating CmrA-catalyzed reduction of
313 TMM*k* affording TMM.

314

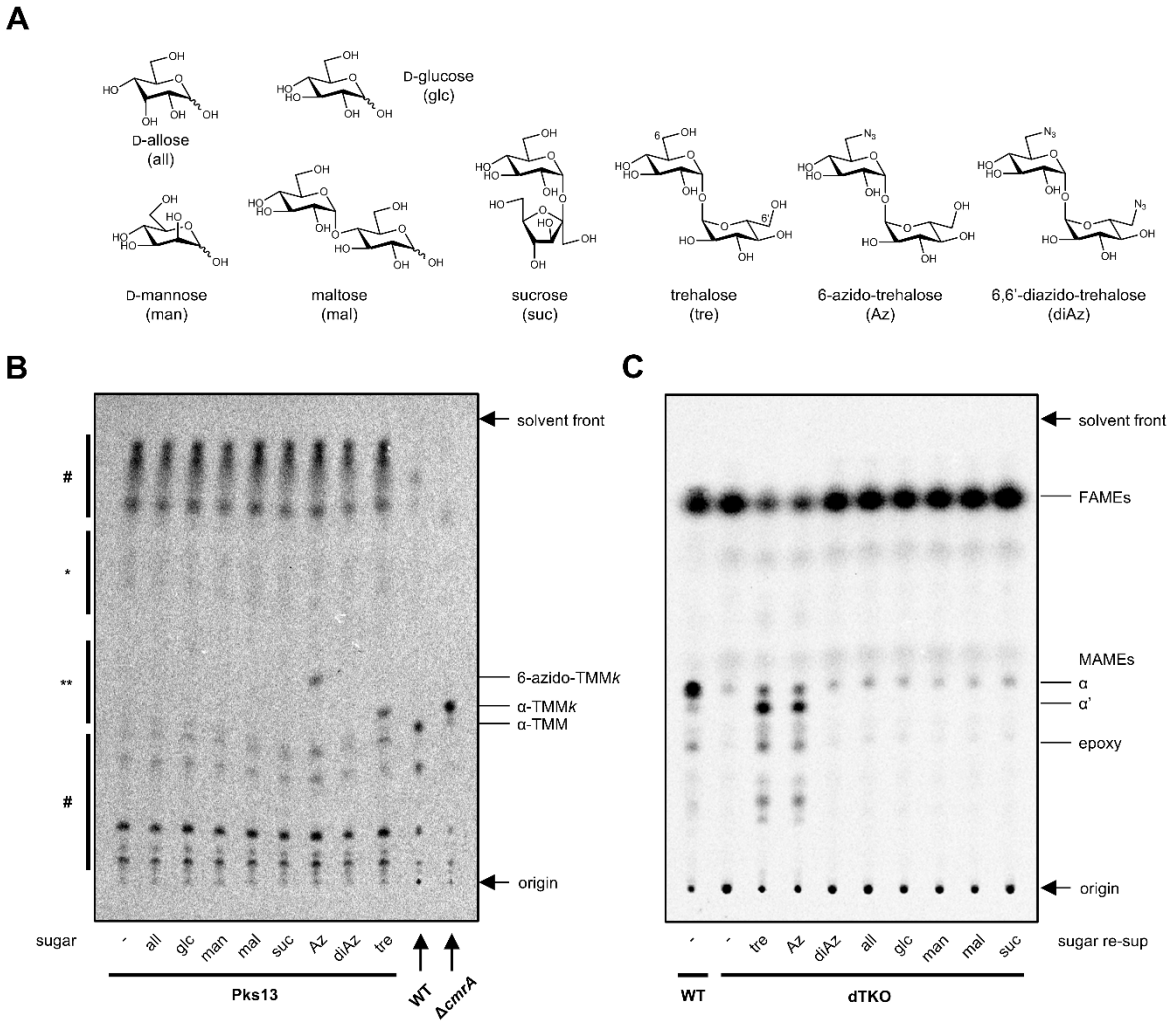

Figure 5. Pks13 specifically uses trehalose to esterify MAs. (*A*) Chemical structures of sugars tested. (*B*) TLC analysis of lipids extracted from the same amount of affinity-purified Pks13-His incubated with the indicated sugar. Total extractable lipids from WT and Δ*cmrA* cells were used as references for migration positions of TMM and TMM*k*, respectively. The top and bottom spots (#) on the TLC are likely non-specifically bound to TALON resin used for affinity purification of the protein. *, a region where monosaccharide monomycolates are expected to appear; **, a region where disaccharide monomycolates are expected to appear. (*C*) TLC analysis of [^{14}C]-labeled total acyl methyl esters derived from dTKO cells re-supplemented with the indicated sugar. Developing solvent: three times in hexane:ethyl acetate 95:5. The TLC plates were visualized by phosphor imaging.

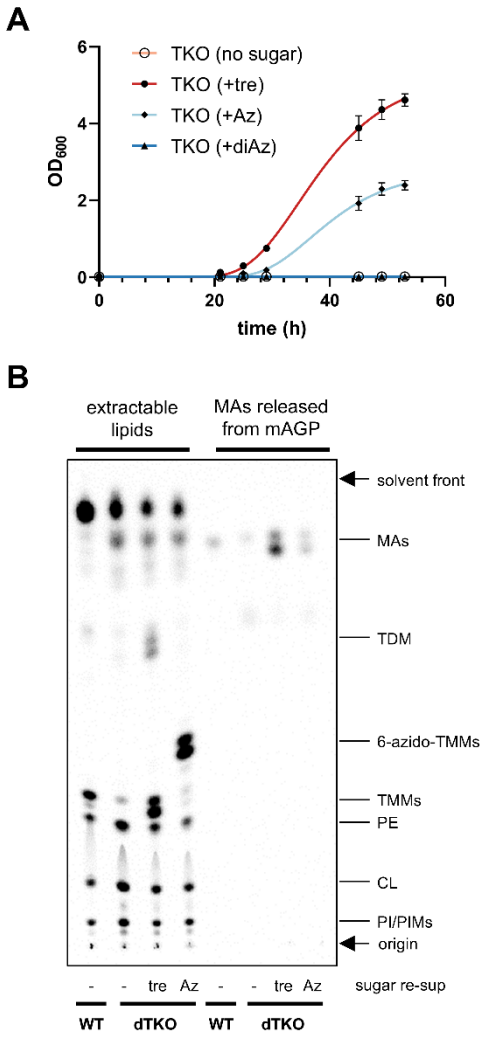

Figure 6. TDM is not required for mycobacterial growth in vitro. (*A*) Growth curves of TKO cells in the presence of the indicated trehalose analogs. TKO cells were depleted of trehalose before subculture into fresh medium (no sugar) or that containing 5 μM trehalose (+tre), 6-azido-trehalose (+Az) or 6,6'-diazido-trehalose (+diAz). Each data point (mean ± SD) represents the results from three biological replicates. (*B*) TLC analysis of [^{14}C]-labeled lipids extracted from trehalose-depleted (dTKO) cells re-supplemented with trehalose (tre) or 6-azido-trehalose (Az). TMMs and TDMs are fully extracted from cells, while MAs conjugated as mAGP were released by base hydrolysis. Developing solvent: chloroform:methanol:water 30:8:1. The same amount of radioactivity was loaded for each extractable lipid sample, while MAs released from mAGP were loaded in the same volume as extractable lipids from the same cells. The TLC plate was visualized by phosphor imaging.

335 **References**

336 1. World Health Organization, Global Tuberculosis Report 2023 (2024).

337 2. V. N. Dahl *et al*., Global trends of pulmonary infections with nontuberculous mycobacteria: a systematic
338 review. *Int. J. Infect. Dis.* **125**, 120-131 (2022).

339 3. C. Hoffmann, A. Leis, M. Niederweis, M. Plitzko Jr., H. Engelhardt, Disclosure of the mycobacterial outer
340 membrane: Cryo-electron tomography and vitreous sections reveal the lipid bilayer structure. *Proc. Natl.*
341 *Acad. Sci. U. S. A.* **105**, 3963-3967 (2008).

342 4. B. Zuber *et al*., Direct visualization of the outer membrane of mycobacteria and corynebacteria in their
343 native state. *J. Bacteriol.* **190**, 5672-5680 (2008).

344 5. P. J. Brennan, D. C. Crick, The cell-wall core of *Mycobacterium tuberculosis* in the context of drug
345 discovery. *Curr. Top. Med. Chem*. **7**, 475-488 (2007).

346 6. M. D. Collins, M. Goodfellow, D. E. Minnikin, A survey of the structures of mycolic acids in
347 *Corynebacterium* and related taxa. *J. Gen. Microbiol*. **128**, 129-149 (1982).

348 7. C. E. Barry III *et al*., Mycolic acids: structure, biosynthesis and physiological functions. *Prog. Lipid. Res.*
349 **37**, 143-179 (1998).

350 8. H. Marrakchi, M. A. Lanéelle, M. Daffé, Mycolic acids: structures, biosynthesis, and beyond. *Chem. Biol.*
351 **21**, 67-85 (2014).

352 9. D. Portevin *et al*., A polyketide synthase catalyzes the last condensation step of mycolic acid biosynthesis
353 in mycobacteria and related organisms. *Proc. Natl. Acad. Sci. U. S. A.* **101**, 314-319 (2004).

354 10. D. J. Lea-Smith *et al*., The reductase that catalyzes mycolic motif synthesis is required for efficient
355 attachment of mycolic acids to arabinogalactan. *J. Biol. Chem*. **282**, 11000-11008 (2007).

356 11. S. Gavalda *et al*., The polyketide synthase Pks13 catalyzes a novel mechanism of lipid transfer in
357 mycobacteria. *Chem. Biol.* **21**, 1660-1669 (2014).

358 12. Z. Xu, V. A. Meshcheryakov, G. Poce, S. -S. Chng, MmpL3 is the flippase for mycolic acids in
359 mycobacteria. *Proc. Natl. Acad. Sci. U. S. A.* **114**, 7993-7998 (2017).
360 13. J. T. Belisle *et al*., Role of the major antigen of *Mycobacterium tuberculosis* in cell wall biogenesis. Science
361 **276**, 1420-1422 (1997).
362 14. A. Banerjee *et al*., *inhA*, a gene encoding a target for isoniazid and ethionamide in *Mycobacterium*
363 *tuberculosis*. Science **263**, 227-230 (1994).
364 15. P. J. Woodruff *et al*., Trehalose is required for growth of *Mycobacterium smegmatis*. *J. Biol. Chem.* **279**,
365 28835-28843 (2004).
366 16. R. Banerjee, P. Vats, S. Dahale, S. M. Kasibhatla, R. Joshi, Comparative genomics of cell envelope
367 components in mycobacteria. *PLoS One* **6**, e19280 (2011).
368 17. M. J. Sartain, D. L. Dick, C. D. Rithner, D. C. Crick, J. T. Belisle, Lipidomic analyses of *Mycobacterium*
369 *tuberculosis* based on accurate mass measurements and the novel "Mtb LipidDB". *J. Lipid. Res*. **52**, 861-
370 872 (2011).
371 18. I. Matsunaga *et al*., Mycolyltransferase-mediated glycolipid exchange in mycobacteria. *J. Biol. Chem.* **283**,
372 28835-28841 (2008).
373 19. F. Miah *et al*., Flux through trehalose synthase flows from trehalose to the alpha anomer of maltose in
374 mycobacteria. *Chem. Biol.* **20**, 487-493 (2013).
375 20. K. A. L. D. Smet, A. Weston, I. N. Brown, D. B. Young, B. D. Robertson, Three pathways for trehalose
376 biosynthesis in mycobacteria. *Microbiology* **146**, 199-208 (2000).
377 21. R. Kalscheuer, B. Weinrick, U. Veeraraghavan, G. S. Besra, W. R. Jacobs, Jr., Trehalose-recycling ABC
378 transporter LpqY-SugA-SugB-SugC is essential for virulence of *Mycobacterium tuberculosis*. *Proc. Natl.*
379 *Acad. Sci. U. S. A.* **107**, 21761-21766 (2010).
380 22. A. Bhatt, L. Kremer, A. Z. Dai, J. C. Sacchettini, W. R. Jacobs, Jr., Conditional depletion of KasA, a key

381 enzyme of mycolic acid biosynthesis, leads to mycobacterial cell lysis. *J. Bacteriol.* **187**, 7596-7606
382 (2005).
383 23. C. Lefebvre *et al*., HadD, a novel fatty acid synthase type II protein, is essential for alpha- and epoxy-
384 mycolic acid biosynthesis and mycobacterial fitness. *Sci. Rep.* **8**, 6034 (2018).
385 24. Y. T. Tsai, V. Salzman, M. Cabruja, G. Gago, H. Gramajo, Role of long-chain acyl-CoAs in the regulation
386 of mycolic acid biosynthesis in mycobacteria. *Open Biol*. **7**, 170087 (2017).
387 25. H. I. Boshoff *et al*., The transcriptional responses of *Mycobacterium tuberculosis* to inhibitors of
388 metabolism: novel insights into drug mechanisms of action. *J. Biol. Chem.* **279**, 40174-40184 (2004).
389 26. D. Alland, A. J. Steyn, T. Weisbrod, K. Aldrich, W. R. Jacobs, Jr, Characterization of the *Mycobacterium*
390 *tuberculosis iniBAC* promoter, a promoter that responds to cell wall biosynthesis inhibition. *J. Bacteriol.*
391 **182**, 1802-1811 (2000).
392 27. A. Bhatt, A. K. Brown, A. Singh, D. E. Minnikin, G. S. Besra, Loss of a mycobacterial gene encoding a
393 reductase leads to an altered cell wall containing beta-oxo-mycolic acid analogs and accumulation of
394 ketones. *Chem. Biol.* **15**, 930-939 (2008).
395 28. N. J. Agard, J. A. Prescher, C. R. Bertozzi, A strain-promoted [3+2] azide-alkyne cycloaddition for
396 covalent modification of biomolecules in living systems. *J. Am. Chem. Soc.* **126**, 15046-15047 (2004).
397 29. K. J. Welsh, R. L. Hunter, J. K. Actor, Trehalose 6, 6'-dimycolate—A coat to regulate tuberculosis
398 immunopathogenesis. *Tuberculosis* **93**, S3-S9 (2013).
399 30. M. E. Horsman, T. P. Hari, C. N. Boddy, Polyketide synthase and non-ribosomal peptide synthetase
400 thioesterase selectivity: logic gate or a victim of fate? *Nat. Prod. Rep*. **33**, 183-202 (2016).
401 31. M. H. Touchette, J. C. Seeliger, Transport of outer membrane lipids in mycobacteria. *Biochim. Biophys.*
402 *Acta* **1862**, 1340-1354 (2017).
403 32. L. E. Quadri, Biosynthesis of mycobacterial lipids by polyketide synthases and beyond. *Crit. Rev. Biochem*.

404 *Mol. Biol.* **49**, 179-211 (2014).

405 33. R. Wilson *et al*., Antituberculosis thiophenes define a requirement for Pks13 in mycolic acid biosynthesis.
406 *Nat. Chem. Biol*. **9**, 499-506 (2013).

407 34. W. Zhang *et al*., Identification of novel coumestan derivatives as Polyketide Synthase 13 inhibitors against
408 *Mycobacterium tuberculosis*. *J. Med. Chem*. **61**, 791-803 (2018).

409 35. A. Aggarwal *et al*., Development of a novel lead that targets *M. tuberculosis* Polyketide Synthase 13. *Cell*
410 **170**, 249-259 (2017).

411 36. C. Khosla, Structures and mechanisms of polyketide synthases. *J. Org. Chem*. **74**, 6416-6420 (2009).

412 37. Y. Yamaryo-Botte *et al*., Acetylation of trehalose mycolates is required for efficient MmpL-mediated
413 membrane transport in *Corynebacterineae*. *ACS Chem. Biol*. **10**, 734-746 (2015).

414 38. T. Clairfeuille *et al*., Structure of the essential inner membrane lipopolysaccharide–PbgA complex. *Nature*
415 **584**, 479-483 (2020).

416 39. C. Silva, S. Ekizlerian, R. Fazioli, Role of cord factor in the modulation of infection caused by
417 mycobacteria. *Am. J. Pathol*. **118**, 238 (1985).

418 40. J. Indrigo, J. Robert L. Hunter, J. K. Actor, Influence of trehalose 6,6'-dimycolate (TDM) during
419 mycobacterial infection of bone marrow macrophages. *Microbiology* **148**, 1991-1998 (2002).

420 41. R. L. Hunter, L. Armitige, C. Jagannath, J. K. Actor, TB Research at UT-Houston—A review of cord factor:
421 new approaches to drugs, vaccines and the pathogenesis of tuberculosis. *Tuberculosis* **89**, S18-S25 (2009).

422 42. R. Ryll, Y. Kumazawa, I. Yano, Immunological properties of trehalose dimycolate (cord factor) and other
423 mycolic acid-containing glycolipids—a review. *Microbiol. Immunol*. **45**, 801-811 (2001).